Check for updates

Optimization of a silver-nanoprism conjugated with 3,3′,5,5′-tetramethylbenzidine towards easy-to-make colorimetric analysis of acetaldehyde: a new platform towards rapid analysis of carcinogenic agents and environmental technology†

Fatemeh Farshchi,[a] Arezoo Saadati,[b] Mohammad Hasanzadeh, [ID] *[cd] Yuqian Liu [ID] [e] and Farzad Seidi [ID] *[e]

Acetaldehyde acts as an important mediator in the metabolism of plants and animals; however, its abnormal level can cause problems in biological processes. Although acetaldehyde is found naturally in many organisms, exposure to high concentrations can have effects on the eyes, respiratory system, *etc*. Due to the importance of detecting acetaldehyde in environmental samples and biofluids, determination of its concentration is highly demanded. There are some reports showing exposure to high concentrations of acetaldehyde for a long time can increase the risk of cancer by reacting with DNA. In this work, we presented a novel colorimetric method for rapid and sensitive detection of acetaldehyde with high reproducibility using different AgNPs with various morphologies. The redox reaction between AgNPs, 3,3′,5,5′-tetramethylbenzidine (TMB) solution, and analytes endows a color change in 15 minutes that is detectable by the naked eye. UV spectrophotometry was further used for quantitative analysis. An iron mold with a hexagonal pattern and liquid paraffin were also used to prepare the paper-based microfluidic substrate, as a low cost, accessible, and rapid detection tool. Different types of AgNPs showed different lower limits of quantification (LLOQ). The AgNPs-Cit and AgNPrs could identify acetaldehyde with linear range of 10^{-7} to 10 M and an LLOQ of 10^{-7} M. The AgNWs showed the best color change activity with a linear range 10^{-5} to 10 M and the lowest diagnostic limit is 10^{-5} M. Finally, analysis of human biofluids as real samples were successfully performed using this system.

1. Introduction

Nowadays one of the main concerns related to human life safety is environmental pollution.[1] Contaminants in food and air can endanger the health of humans and all living organisms, so the rapid identification and detection of these toxic and carcinogenic compounds can be effective factors in protecting the

[a]*Fundação Oswaldo Cruz, Instituto Oswaldo Cruz, Laboratório de Biologia Molecular e Doenças Endêmicas, Avenida Brasil No 4365 – Manguinhos, Rio de Janeiro 21040-900, RJ, Brazil*

[b]*Central European Institute of Technology, Brno University of Technology, Brno CZ-612 00, Czech Republic*

[c]*Pharmaceutical Analysis Research Center, Tabriz University of Medical Sciences, Tabriz, Iran. E-mail: hasanzadehm@tbzmed.ac.ir*

[d]*Nutrition Research Center, Tabriz University of Medical Sciences, Tabriz, Iran*

[e]*Jiangsu Co-Innovation Center for Efficient Processing and Utilization of Forest Resources and International Innovation Center for Forest Chemicals and Materials, Nanjing Forestry University, Nanjing, 210037, China. E-mail: f_seidi@njfu.edu.cn*

† Electronic supplementary information (ESI) available. See DOI: https://doi.org/10.1039/d3ra00355h

health of living organisms.[2] Acetaldehyde is a flammable liquid and its pungent odor is naturally present in various plants, mature fruits, vegetables, cigarette smoke, and smoke from gasoline and diesel fuel.[3,4] This compound acts as a mediator in the metabolism of plants and animals and its amount is not visibly detectable.[5] A high amount is involved in biological processes. Due to its role in alcohol fermentation processes, it is found in small amounts in all alcoholic beverages.[6] Although acetaldehyde is found naturally in many organisms, exposure to high concentrations can have effects on the eyes, respiratory system, and *etc*.[7,8] While there is no exact information about the relationship between this substance and cancer, there are some reports that exposure to high concentrations of acetaldehyde for a long time can increase the risk of cancer by reacting with DNA.[9–11] High Performance Liquid Chromatography (HPLC) based methods have been used for detection of acetaldehyde.[12] Also, gas chromatography (GC) and high-performance liquid chromatography (HPLC) can provide suitable sensitivities.[13] Although these methods have good diagnostic ability, they are

complex and time-consuming processes. In this way, Ghica *et al.*, developed an electrochemical biosensor for detection of acetaldehyde using acetaldehyde dehydrogenase.[14] In this study, acetaldehyde is converted to acetate oxide using the enzyme which has low accuracy.

Colorimetric sensors based on using nanoparticles have been widely studied for this purpose.[15–17] These methods are very simple compared to other techniques and do not require complex and high-costs tools.[18] Nanoparticles lead to increase the accuracy and sensitivity of these sensors.[19] Nanoparticles show very good properties depending on their level of aggregation, which is mostly determined by specific surface plasmon resonance (SPR) profiles.[20] Due to their small size, metal nanoparticles can limit their electrons and cause a quantum effect.[21,22] Reducing the particle size also increases the catalytic properties and increases the surface-to-volume ratio.[23] This is an important principle for using metal nanoparticles in colorimetric sensors that can compete with analytical techniques such as fluorescence or absorption.[24] These nanoparticles can be easily used to identify proteins, enzymes, metal ions, small molecules, and DNA.[25]

The integration of new and advanced sensors on microfluidic substrates promises new and advanced systems that can be commercialized as diagnostic kits.[24] This system consists of channels that can work well in analytics detection.[26] It can also be engineered on the surface of the paper.[27,28] These types of sensors allow the simultaneous detection of several analytes at the same time.[29,30] One of the popular and famous methods is using a printer to make a particular pattern on the wax screen and PDMS (polydimethylsiloxane).[27] The use of these techniques is costly and requires advanced devices and equipment. Among these, the simplest method is to use paraffin and iron pattern, which have high flexibility and easy construction.[31] These papers are also disposable and can be commercialized due to their production at a very low price.[32]

In this work, we designed a novel paper-based microfluidic substrate toward identification of acetaldehyde. This system works based on color change, which can easily detect the target molecule by naked eye. UV spectrophotometers were also used for quantitative analysis of acetaldehyde. This spectroscopic method using AgNPs was very efficient and effective to increase the accuracy and sensitivity of the system. AgNPs have high catalytic activity and high electron density.[33–35] AgNPs are low toxic nanoparticles and stable and they are not sensitive to light.[36] This system is innovative and biocompatible.

3,3′,5,5′-Tetramethylbenzidine (TMB) is a chromogenic substrate used in staining procedures in immunohistochemistry as well as a visualization reagent used in enzyme immunoassays (ELISA).[37] The mechanism of TMB oxidation by HRP/ H_2O_2 is a well-known process described by Josephy *et al.*[38] Oxidation of TMB by H_2O_2 first gives a complex product with blue color, which is changed to another color after adding the probe (AgNPs) and analyte (acetaldehyde) to the reaction medium. The TMB solution has an absorbance peak at 450 nm and it is also electrically active thus allowing electrochemical detection.[39] Silver nanoparticles due to their peroxidase properties in combination with TMB cause better color change and increased sensitivity.[40] Silver nanoparticles also have great stability and surface area.[41] Acetaldehyde changes colors of optical probes (AgNPs) due to the accumulation of nanoparticles based on binding of analytes with probe. Liquid paraffin was used to prepare microfluidic papers. Based on our previous experiment papers were the best choice.[33,34] The hot iron pattern was pushed on the paraffin-immersed paper, paraffin-free paper, and a strong magnet, with this technique, hydrophilic channels, and hydrophobic areas were created on the surface of the paper. This technique is low-cost, easy, portable, and fast (takes around 3 minutes). Based on the obtained results, the proposed colorimetric paper-based microfluidic sensor is innovative and has a good response to acetaldehyde in human urine samples.

2. Experimental

2.1. Chemicals and materials

Ethylene glycol (EG), silver chloride (AgCl), polyvinyl pyrrolidone (PVP K-30), hydrogen peroxide (H_2O_2), triethylamine, 3,3′,5,5′-tetramethylbenzidine (TMB), sodium borohydride ($NaBH_4$), sodium hydroxide (NaOH), acetic acid (CH_3COOH), potassium iodide (KI), hydrogen tetrachlorocuprate(III) hydrate ($HAuCl_4 \cdot 3H_2O$), silver nitrate ($AgNO_3$), tri-sodium citrate ($Na_3C_6H_5O_7$), formaldehyde and acetaldehyde were bought from Sigma Aldrich (Ontario, Canada).

2.2. Synthesis of nanoparticles

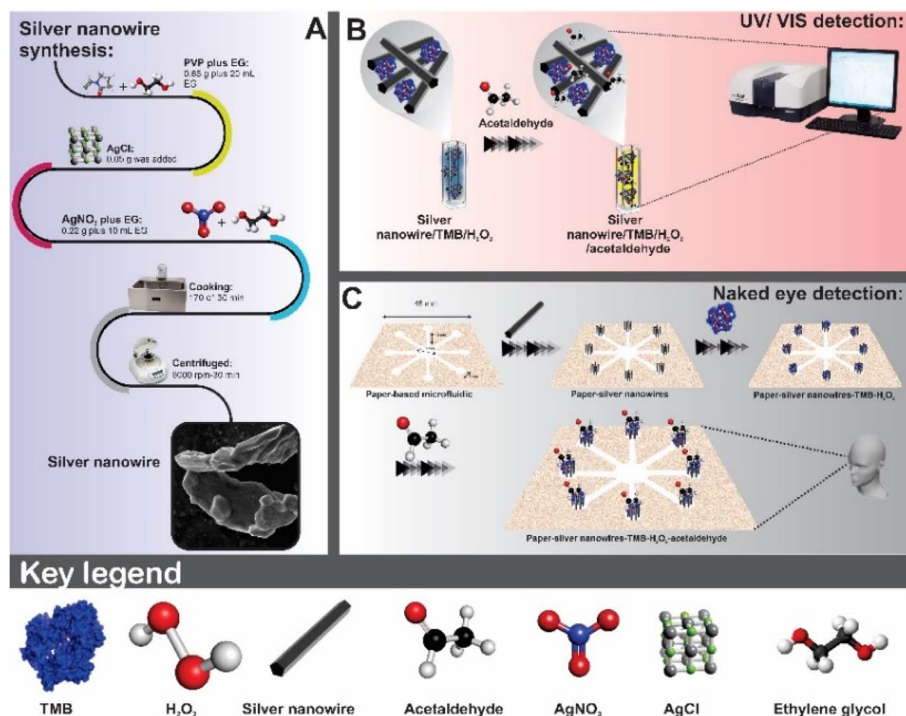All of the AgNPs were synthesized according to our previous reports.[33,34]

2.3. Procurement of colorimetric sensor for detection of acetaldehyde

For this purpose, various types of AgNPs with different morphologies were used as a probe and mixed with the bluish-green combination of TMB and H_2O_2 (in a volume ratio of 1 : 1) solution. The TMB solution in the presence of H_2O_2 oxidizes to bluish-green. On the other hand, AgNPs works as peroxide and change the NPs color. Also, a saturated solution of acetaldehyde was mixed with the bluish-green solution at room temperature and because of oxidation, the color was changed. Different concentration of acetaldehyde was also organized using DW for more examination. The color changes were confirmed by UV-vis spectrophotometry as quantitatively analysis regime (Scheme 1).

2.4. Production of microfluidic paper-based sensor

The proposed pattern containing 8 hydrophilic circular zones was designed using CorelDRAW software. Circular diagnostic zones (diameter 5 mm) are connected to microfluidic channels (length 10 mm and width 30 mm) and the central zone (diameter 10 mm) to the input sample. In this way, the papers have immersed in molten paraffin for 30 s. Then take them out and let the paraffin dry on paper for 1 minute. In the next step, the paraffin-free paper was put under the paraffin paper on the surface of a very strong magnet. Then, a hot 8-pronged iron

Scheme 1 Schematic illustration of the preparation of paper-based microfluidic sensor for the identification of acetaldehyde by using AgNWs. (A) Described the AgNWs synthesis process, (B) UV-vis detection of acetaldehyde by using AgNWs, (C) detection of acetaldehyde on the surface of the prepared paper-based microfluidic sensor.

pattern ($t = 150$ °C) was used as a stamp on the papers. The absorption between the magnet and the iron pattern helps to create hydrophilic channels and hydrophobic areas on the paraffin-free paper easily. The steps for the substrate preparation are shown in Fig. 1.

2.5. Apparatus

Colorimetric detection was investigated with the smart phone camera (iPhone 12 ProMax,12 megapixels). The images were recorded under natural light sources. UV-vis spectrophotometer Shimadzu UV-1800 with a resolution of 1 nm was employed to study the optical examination. AFM (atomic force microscope) was attained by Nano surf (AG Gräubernstrasse 124 410 Liestal Switzerland) system. Field emission scanning electron microscope (FE-SEM) Hitachi SU8020, Czech with a 3 kV powerful voltage and high resolution was used to study the morphology of synthesized nanoparticles. Energy scattering spectroscopy (EDS) was used to study the chemical elements. Dynamic light scattering (DLS) (Zetasizer Ver. 7.11, MAL1032660, England) was employed to measurement the size distribution and zeta potential of prepared nanoparticles.

2.6. Identification of acetaldehyde using the optical method

To study the performance of AgNPs along with TMB toward interaction with acetaldehyde and in the mixture of bluish-green TMB and acetaldehyde, a UV-vis spectrophotometer was used. In this way, AgNPs, TMB and acetaldehyde were mixed in a 1 : 1 : 1 volume ratio at room temperature and were

immediately examined and evaluated on the UV-vis spectrophotometer.

3. Results and discussion

In this study, the efficiency of AgNPs based colorimetric chemosensors and paper-based microfluidic arrays for acetaldehyde detection were evaluated. Because these types of nanoparticles show the absorption peak in the visible wavelength range, they are suitable for optical identification analytes like acetaldehyde.

3.1. UV-vis spectroscopic

Anisotropic noble metal nanoparticles have the extraordinary structural, surface, and photonic properties that have attracted much attention in optical chemosensors today.[35–50] Nanomaterials, such as metal nanoparticles, are identified by their different physical and chemical properties.[51] These characteristics are directly proportional to the surface/volume ratio. The surface-to-volume ratio increases as the particle size decreases and the surface area increases. Therefore, surface atoms and molecules play an important role in nanoparticles and influence the properties of nanoparticles.[52,53] Among the physical and chemical qualities, optical properties are of particular importance and are often used in simple and rapid measurement methods.[54] The interaction of light with nano systems leads to certain events such as transmission, absorption, reflection, light scattering, transmission, and fluorescence.[55]
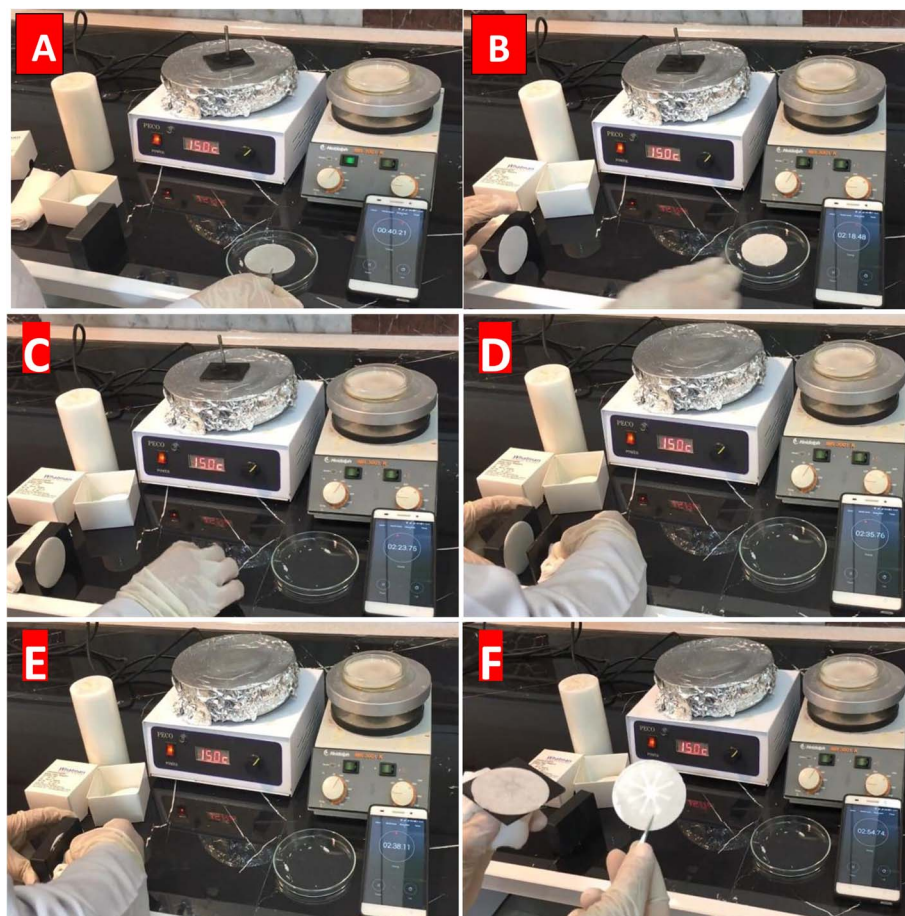
Fig. 1 The fabrication process of microfluidic paper-based sensor, (A) involvement of paper in molten paraffin, (B) drying step of paraffin on paper, (C) put paraffin-free and paraffin-free paper on the magnet (D) place the hot iron pattern on the paper and the magnet, (E) place the hot iron pattern on the paper and the magnet, (F) prepared microfluidic substrate.[33,34]

For example, AgNPs detected by specific absorption bands have a certain intensity, but the binding properties change due to changes in the external environment or exposure to the analyte.[56] This sensitivity to the external environment can be used in the field of optical chemical detection of specific analytes. When the light beam hits the solution, surface plasmons occur, which indicates the presence of nanoparticles and leads to a sharp peak in the visible region.[57] Localized surface plasmon resonance is a phenomenon specific to metal nanoparticles, especially silver nanoparticles, and depends on the dielectric constant of its surroundings. Because of their free electrons, AgNPs produce a luminous effect known as surface plasmon absorption banding, which is the result of the composite oscillations of the electron nanoparticles in the resonance of the wave light in a water suspension.[58,59] Increasing the size of the nanoparticles causes the plasmon absorption to shift to a lower energy wavelength and appear red.[60] In addition, the absorption peak becomes wider indicating suspension growth and agglomeration formation. The presence of the analyte results in a constant dielectric change, appearing as a color change and a change in the position and intensity of absorption.[61] In this study, the colorless TMB solution was oxidized in the presence of H_2O_2 and then reduced in the presence of the analyte, which leads to the identification and discoloration of the analyte. The AgNPs in this section act as a strong catalyst and increase the oxidation rate of TMB. Indeed, the nanoparticles have a function similar to peroxidase, and H_2O_2 decomposes into OH radicals, and the resulting radicals increase the oxidation of TMB. So, optical performance of AgNPs with various morphologies towards identification of acetaldehyde was studied by UV-vis. Since the smaller colloidal particles can absorb visible light through the movement of the SPR, capping or stabilizing agents can be used to prevent the nanoparticles from binding or accumulating with other particle components probe.[62] Coating the nanoparticles with additives leads to electrostatic repulsion between them.[63] Silver atoms are closely associated with electron-rich sites because they are among the most efficient atoms. These accumulated negative charges carried across the domain of the nanoparticles have a distinct nature and increase the stability of the nanoparticles.[64] Acetaldehyde can interact strongly with the negative charge of oxygen (OH) in the additive detection probe system and lead to the agglomeration required for colorimetric target identification.

3.1.1 AgNPrs. In this work, silver nanoparticles with different morphologies and TMB as a redox reagent were used for detection of acetaldehyde. The resulting deformation is also seen visually in the color of the solution, allowing acetaldehyde analysis in both the solution and leading to a change of UV-vis spectrum wavelengths. Morphological changes lead to a change in the color of nanoparticles from blue to green, which can be detected by the naked eye.[65] In fact, at the beginning of the AgNPrs interaction with TMB and acetaldehyde, $AgNO_3$ is reduced to Ag atoms deposited on the surface of AgNPrs, converting the AgNPrs to AgNPs. With the addition of acetaldehyde to solution number 3, the adsorption of the solution changes to 450 nm, and the adsorption intensity is constant in the same range of 1000, which indicates the stability of the nanoparticle accumulation. Over time, the redox reaction between the acetaldehyde and silver ions was completed, and the newly formed silver atoms changed the color of the solution to yellow. Electrostatic interactions between the acetaldehyde and the surface of modified detection probes can lead to the accumulation of AgNPs in the solution. After one hour, no change in the color of the AgNPrs probe was observed, while the peak intensity of adsorption not changed too. In the second solution (probe + TMB) and (probe + TMB + analyte), a discoloration was observed in the solution after one hour. Despite discoloration of the detection probe solutions after one hour in the presence of the analyte, no significant changes in the absorption peak intensity of AgNPrs were observed at the 550 nm wavelength.

3.1.2 AgNWs. AgNWs have an anisotropic shape and produce two plasmon bands including a longitudinal plasmon band and a transverse plasmon band (corresponding to the electronic shift along the short axis of the rod). This feature sets them apart for use in a wide range of spectroscopic studies.[66] The performance of AgNWs for optical identification of acetaldehyde was studied using the UV-vis technique. AgNWs show suitable color changes as well as adsorption intensity. Furthermore, the peak of the in-plane dipole resonance is very shape-dependent, which is used to design sensors based on wavelength variation. As shown in Fig. 2(C) and (D), after the addition of TMB, the adsorption intensity decreased due to oxidation. Also, the spectrum shows that the combination of TMB and AgNWs prepared here has three absorption bands located at 650, 450 and 350 nm, respectively. After the addition of acetaldehyde due to reduction, the adsorption intensity increased to 2 nm and the location of the peak was occurred at 450 nm. Finally, it can be said that the prepared solutions have a good ability to detect acetaldehyde. The stability of these nanoparticles and solutions combined with TMB and acetaldehyde was also evaluated after one hour.

3.1.3 AgNPs-Cit. The synthesized solution is light yellow (Fig. 2(E) and (F)), which has a lower absorption intensity due to its low color. The prepared AgNPs-Cit have UV-vis absorption at wavelengths of 400 nm. AgNPs-Cit does not show a good color change and after blending with TMB, it becomes almost colorless. The absorption intensity is also almost zero. After 1 hour, the stability of the nanoparticles also decreases, but the

final composition (AgNPs-Cit + TMB + acetaldehyde), although they had low adsorption intensity, had good stability, and the color change was more pronounced after one hour.

3.2. Analytical study

In this study, the colorimetric method was performed to identify acetaldehyde using the peroxidation activity of AgNPs. UV-vis technique was used to investigate apportion of proposed optical probes toward determination of acetaldehyde (10^{-7} to 10 M) in the presence of silver nanoparticles and TMB solution. The absorption spectrum in the 400–800 nm range is along with the adsorption/concentration ratio are shown in Fig. S1–S3 (see ESI†). Next, important analytical parameters such as linear band properties and lower limit of quantification (LLOQ) obtained from standard curves plotted by the change in absorbance in the 600 nm band at different concentrations of acetaldehyde. According to the obtained results, at high concentrations of acetaldehyde a sharp peak of in-plane dipolar resonance (650 nm) is also observed in the LSPR spectrum, which is accompanied by a change in solution color. This phenomenon can be attributed to changes in the morphology of AgNPrs and the tendency of silver atoms to deposit on their surface.[67] According to the obtained results, using AgNPs-Cit and AgNWs as optical probes, the adsorption intensity decreases with decreasing concentration which can be related to the size of nanoparticles, and in AgNPrs, the adsorption intensity increases with decreasing concentration. Using AgNPrs, by decreasing the concentration of acetaldehyde its performance decreases, and the catalytic activity of nanoparticles with TMB increases. These color changes can also be seen with the naked eye. The linear relationship and regression equation for each type of nanoparticles are plotted and the results are listed in Table 1.

According to Table 1, although all types of investigated AgNPs have great detection limit and LLOQ for the determination of acetaldehyde, for preparing a suitable diagnostic kit, AgNWs is the best choice. This nanoparticle has very clear color changes which can be detected by naked eye. As shown in the above results, using AgNWs the adsorption peaks also decrease with decreasing concentration of acetaldehyde. In summary, AgNWs are the excellent nanoparticles for the optical monitoring of acetaldehyde.

As it is shown in Table 2, we prepared an optical and colorimetric biosensor for acetaldehyde detection. Colorimetric and optical biosensor strategies have great potential for the development of aldehydes like acetaldehyde detection platform technologies. Chemo sensor platforms are attractive for future acetaldehyde detection due to factors such as rapid readout, cost-effectiveness, sensitivity, selectivity, and portability. To the best of our knowledge, there is no report on the detection of acetaldehyde based on the sensing probes introduced in this study, which is one of the benefits of this work. The ability of proposed probes for acetaldehyde examination was evaluated using UV-vis spectroscopic technique. A comparison of the analytical performance of the presented sensor with previous studies shows that this sensor is more
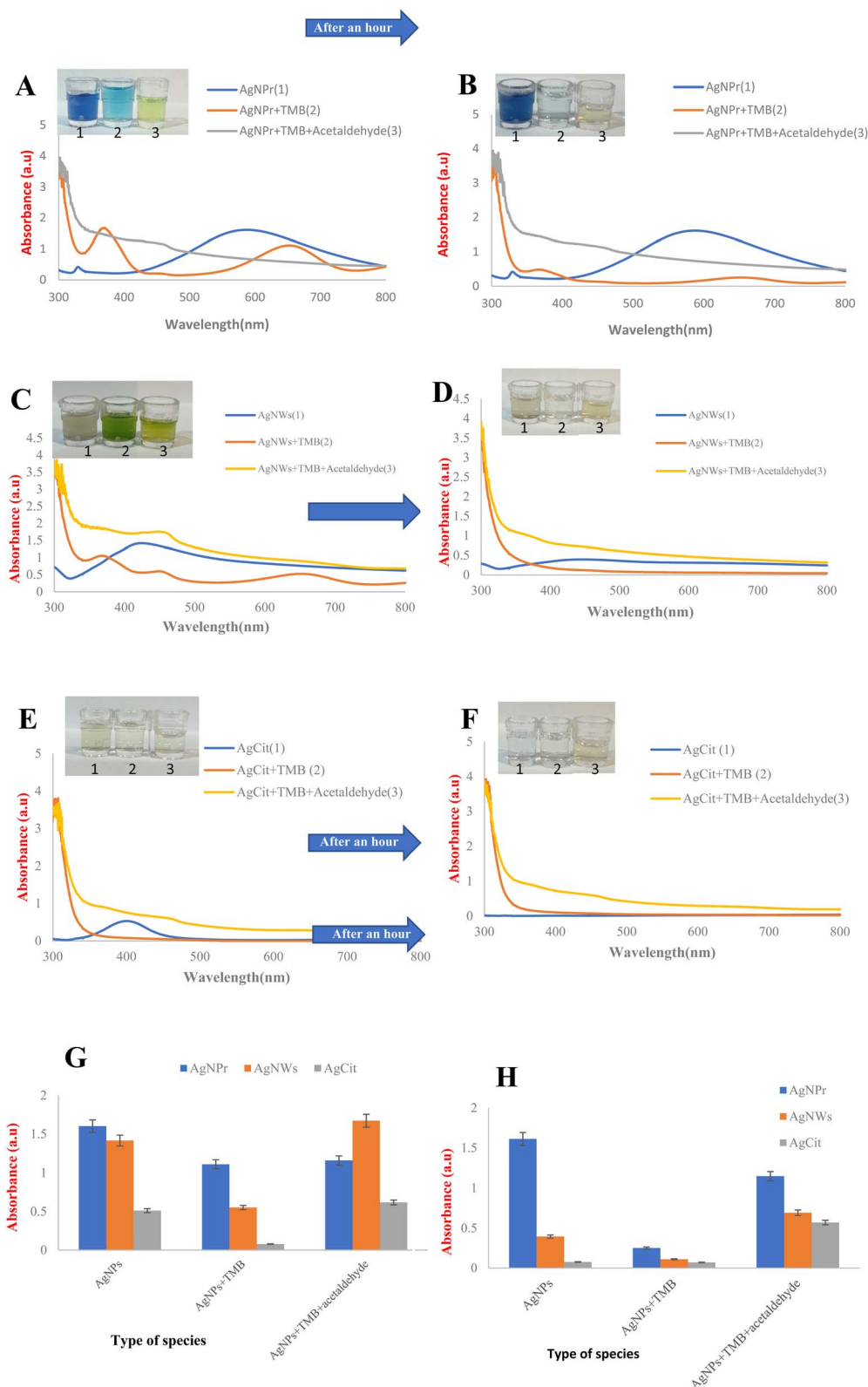
Fig. 2 (A)–(F) UV-vis absorption response of prepared AgNPs in the mixture of acetaldehyde and colorless solution and differential UV-vis absorption response after an hour and photographic image of prepared solutions. Histogram of UV-vis absorption response of synthesized AgNPs and after reaction with acetaldehyde immediately (G) and (H) after an hour ($n = 3$, SD = 2.06).

Table 1 Analytical figure of merits

Type of AgNPs	Linear range (M)	Regression equation	R^2	LLOQ (M)
AgNPrs	10^{-7} to 10 M	Abs (a.u) = $-0.0347 C_{acetaldehyde} + 0.5391$	0.9953	10^{-7}
AgNPs-Cit	10^{-7} to 10 M	Abs (a.u) = $0.014 C_{acetaldehyde} + 0.0344$	0.9017	10^{-7}
AgNWs	10^{-5} to 10 M	Abs (a.u) = $0.0244 C_{acetaldehyde} + 0.7515$	0.9465	10^{-5}

Table 2 Study the presentation of the engineered biosensor for the identification of acetaldehyde

Method	Reaction system	Linear range	LOD/LLOQ	References
Fluorescence spectrometry	Optical fiber probe/ADH	225 to 0.45 μM	0.45 μM	68
Ultraviolet spectrophotometry	AldDH surface displayed whole-cell	1 to 300 μM	0.33 μM	69
Electrochemical	Biofuel cell/alcohol dehydrogenase (ADH)	5 to 200 μM	1 μM	70
	Carbon film electrode/AldDH/NADH oxidase	0 to 60 μM	2.6 μM	71
	Copper electrode in alkaline solution	5.21 to 50 mM	50 mM	12
	Screen-printed biosensor	—	1 μM by amperometry 6 μM by chronoamperometry	72
	Screen-printed graphite electrodes	5 to 500 μmol L^{-1}	1 μmol L^{-1}	73
Colorimetric/UV-vis	AgNPr/TMB-H$_2$O$_2$	1×10^{-7} to 10 M (SD = 2.11)	10^{-7} M (SD = 1.76)	This work
	AgCit/TMB-H$_2$O$_2$	1×10^{-5} to 10 M (SD = 2.55)	10^{-5} M (SD = 2.33)	
	AgNWs/TMB-H$_2$O$_2$	1×10^{-7} to 10 M (SD = 2.40)	10^{-7} M (SD = 2.01)	

sensitive to them and can detect acetaldehyde in a wider linear range. In addition, colorimetric studies were performed using paper-based microfluidics, which indicates the potential performance of these microfluidics in the development of acetaldehyde diagnostic kits. On the other hand, the prepared system is very simple, sensitive, low-cost, affordable, selective, and is not time-consuming. This system is small and portable. Integrating current biosensor platforms into routine clinical use still requires significant advances in future research. To build a universal sensing strategy, we need to integrate electrochemical and optical transmission mechanisms with the merits of different biosensor strategies. We believe that establishing clinical procedures for sample handling is essential for extensive sample analysis. In addition, the integration of detection systems is limited and will require additional developments. Therefore, the study of integrating sensors, recognition factors, and transducers into a storage biosensor product requires more scientific and technological efforts to achieve a system universally applicable mobile point of care. In addition, advances *in vivo* multichannel biosensor strategies are still limited. Once engineering challenges, such as advances in biocompatible materials and *in vivo* multi-signaling, are resolved, next-generation biosensor platforms could become the norm widely used for point-of-care screening and detection systems. In summary, we can say that this optical system is a new way for feature analytical studies.

3.3. UV-vis spectroscopic measurements in real samples

To study the performance of acetaldehyde in the real samples, human urine samples were taken from healthy individuals without any pretreatment. In this way, urine samples were mixed with different concentrations of acetaldehyde (1×10^{-7}–

17.35 M) with a volume ratio of 1:1 V:V. The UV-vis spectrophotometry Fig. S4–S6 (see ESI†) was used to study the adsorption. In the case of AgNWs and AgNPs-Cit adsorption intensity decreases with decreasing the concentration but in AgNPrs it's quite the opposite.

3.4. Selectivity

Selectivity is an important factor in designing a sensor system. To evaluate the selectivity of the prepared chemo sensor, we first combined various interfering agents such as acetone, ethanol, glucose, and formaldehyde separately with the dye and silver solution and examined them. As shown in Fig. 3–6, the best color change and adsorption intensity occurred in the presence of acetaldehyde, which indicates a successful reaction between AgNPrs and detected analyte. In the cases of interfering investigation in the presence of some interferers a shift at the peak of the adsorption band is observed. Changes in the absorption band in different optical probes are different. As can be seen, the prepared AgNPs containing TMB have UV-Agabsorption at wavelengths of 350, 450, and 650 nm. The first two absorption bands (350 and 450 nm) correspond to out-of-plane and in-plane quadrupole resonance of AgNPs, respectively. The 650 nm band is attributed to the AgNPs in-plane dipole resonance. The peak of in-plane bipolar resonance is strongly dependent on the AgNPs shape. This phenomenon, which is used in the design of sensors based on wavelength changes, can be attributed to changes in the morphology of AgNPs and the tendency of newly produced Ag atoms to deposit at the AgNPs surface. In the mixture of AgNPrs with TMB and interferers (GLU/ethanol/acetone and formaldehyde), the adsorption decreases in the 350 nm band and increases in the 650 nm band. In the other AgNPs the adsorption increases in the 350 nm band and decreases in the
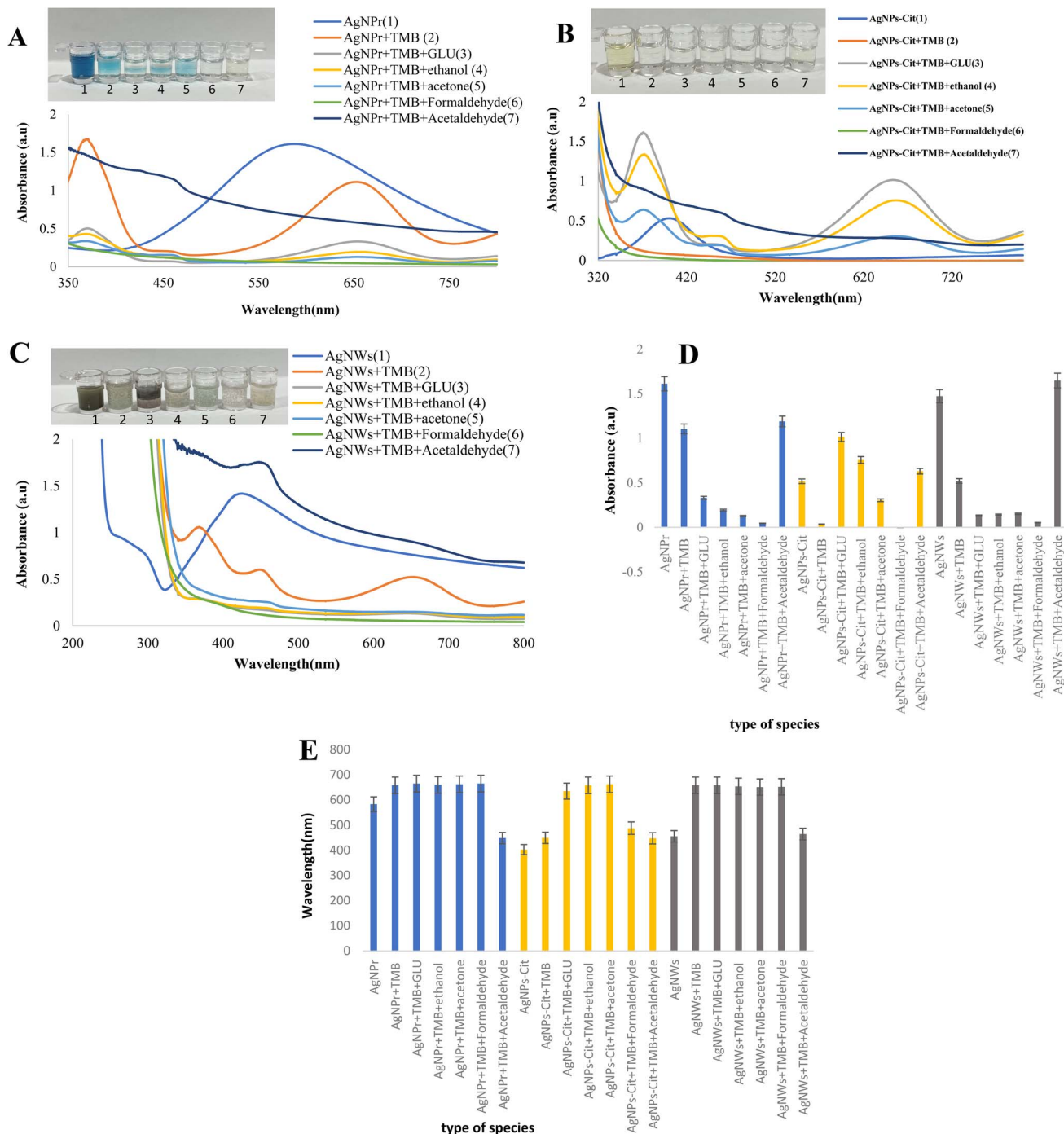
Fig. 3 (A)–(C) UV-vis spectra and colorimetric sensing of the interaction between AgNPs, in the presence of prepared TMB solution and various analytes. Histogram of (D) the intensity of absorption and (E) the wavelength of absorption ($n = 3$, SD = 1.89).

650 nm, these changes can be attributed to the fact that the morphology of sensing probes. Also, acetaldehyde adsorption peak in the presence of AgNPrs with good color change is visible in the range of 450 nm, while in the presence of glucose, ethanol, and acetone, no effective color change can be observed, and most of the appearance of the peaks were due to the effective presence of the dye solution. The same can be seen and discussed in the presence of other silver

nanoparticles, the best performance of which can be attributed to AgNWs and AgNPrs. To further investigate this selectivity in the real urine sample, acetaldehyde in the presence of all three AgNPs had better results than the other analytes. Fig. 3–6 shows the complete histogram related to the change in the location of the peaks, which is also observed in the presence of the target analyte, acetaldehyde, and this is related to the successful redox oxidation reaction.
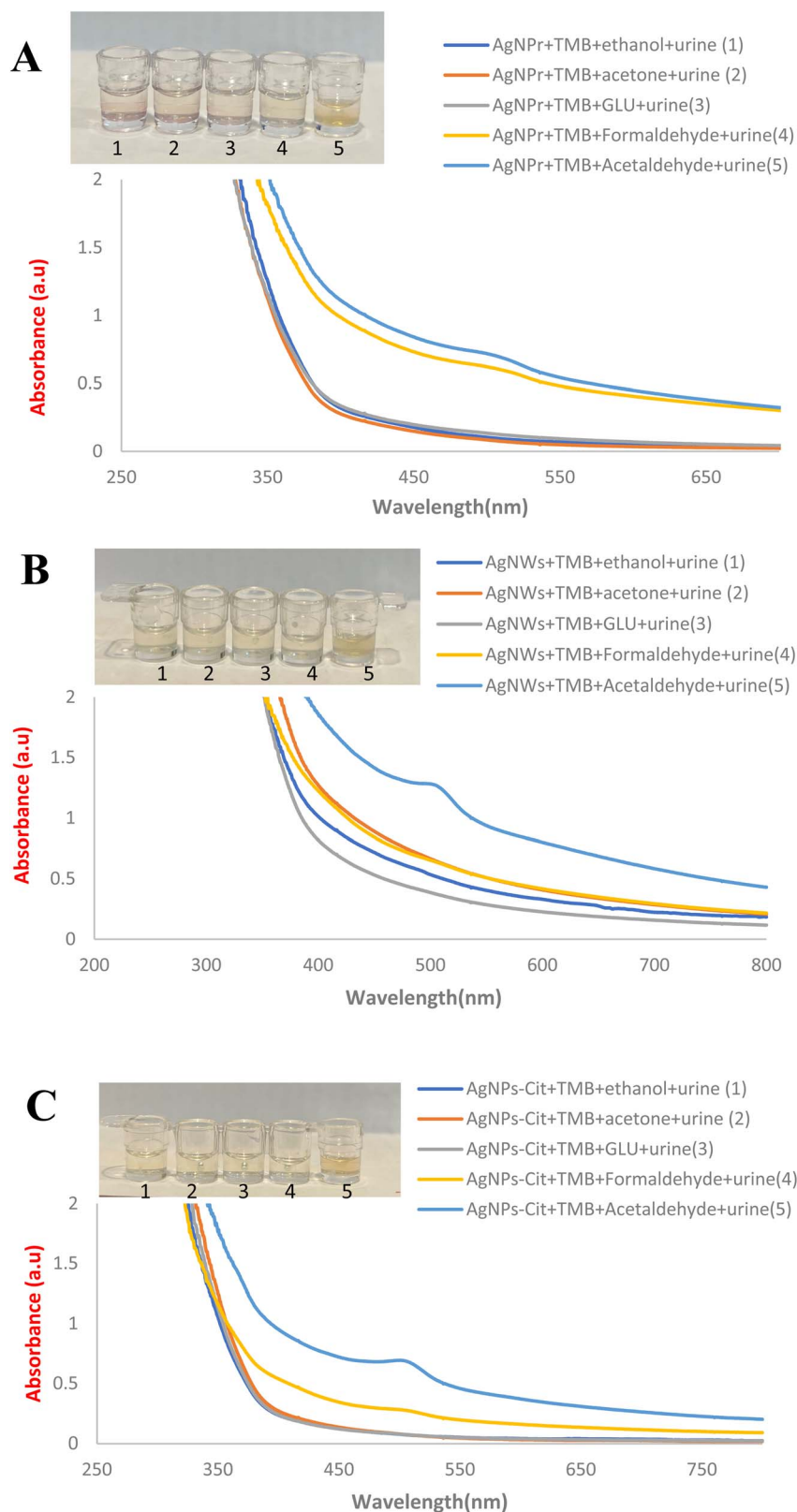
Fig. 4 (A)–(C) UV-vis spectra and colorimetric sensing of the interaction between acetaldehyde and AgNPs, in the presence of prepared TMB solution and various interfering species analytes in real sample.
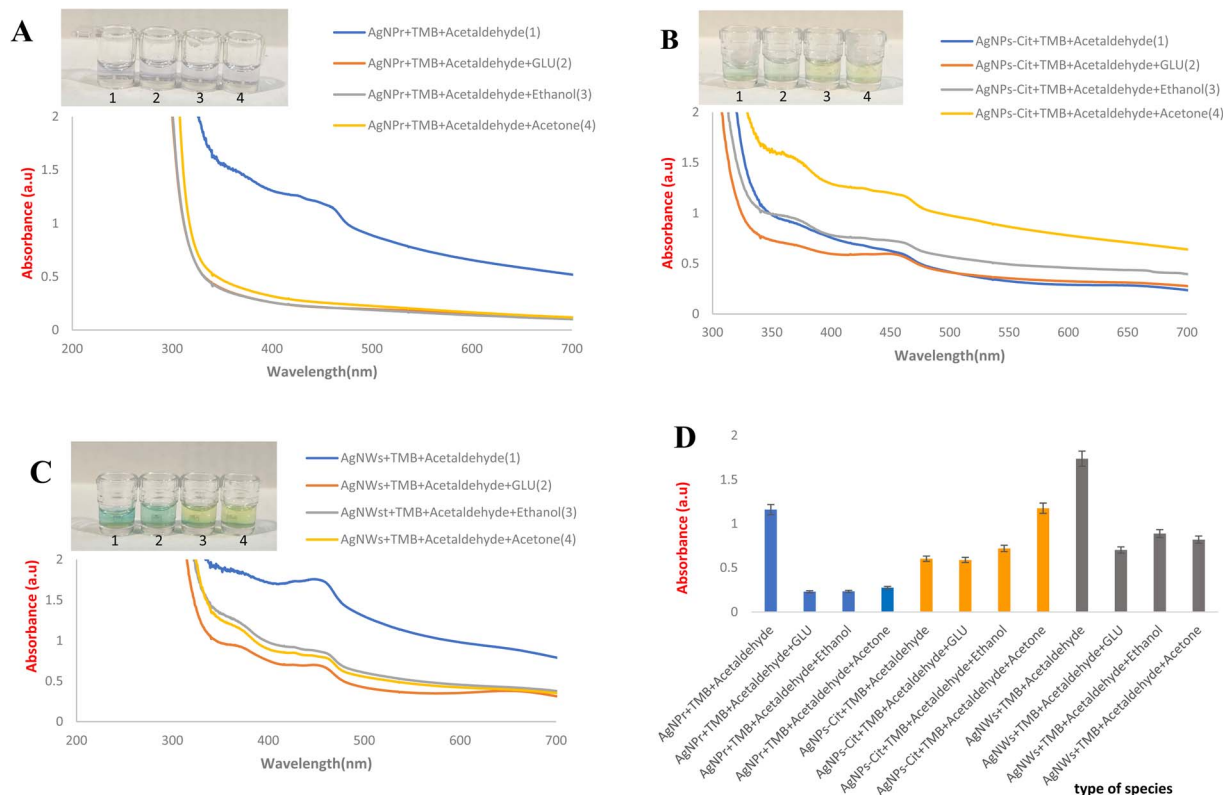
Fig. 5 (A)–(C) UV-vis spectra examines and photographic images of the effect of the interveners in the prepared solution containing AgNPs, TMB and acetaldehyde. (D) Histogram of the intensity of absorption ($n = 3$, SD = 2.32).
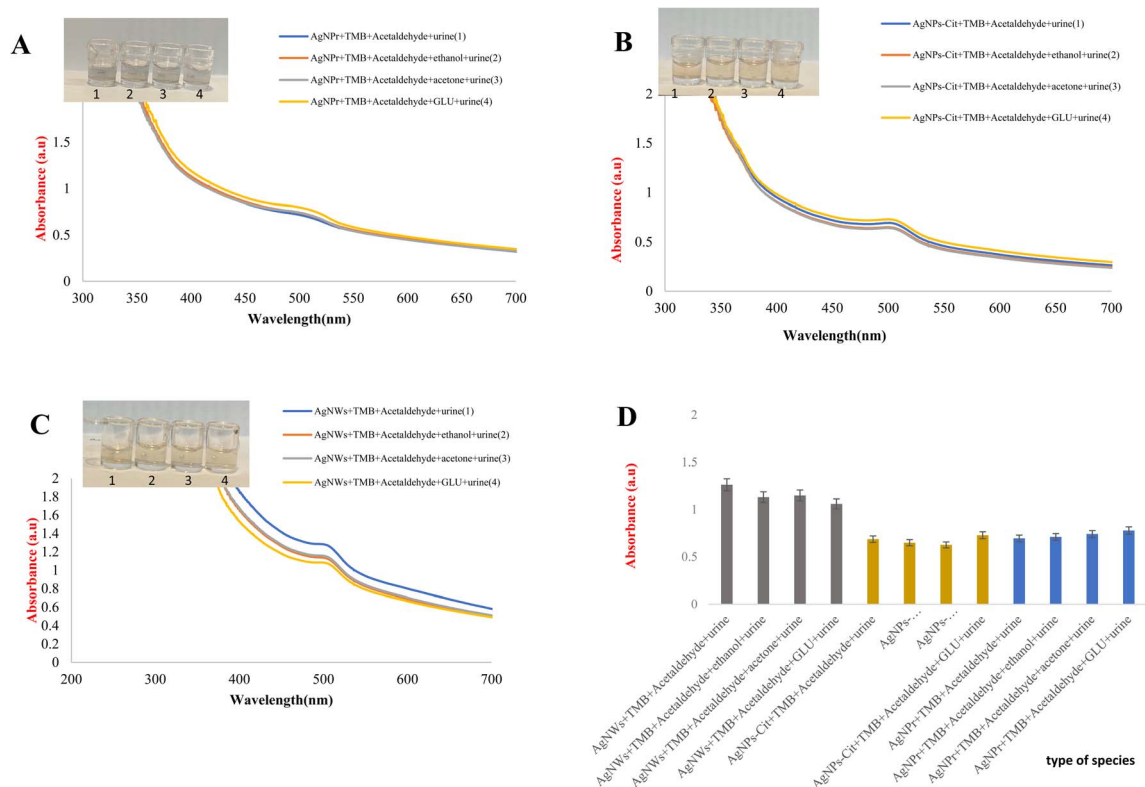

Fig. 6 (A)–(C) UV-vis spectra examines and photographic images of the effect of the interveners in the prepared solution containing AgNPs, TMB and acetaldehyde in real sample. (D) Histogram of the intensity of absorption ($n = 3$, SD = 1.69).

4. Colorimetric detection of acetaldehyde on the surface of engineered papers

In addition to the promising results of UV-vis spectrophotometry, we used paper-based microfluidic as a diagnostic kit for easier examination that can be used outside the laboratory toward real time analysis of chemical, pollutants, markers, and *etc.* In recent studies, paper-based sensors have attracted a lot of attention due to their ease of use and affordable price, and it can be said that they have made great progress.[74,75] This system has a high potential to low-cost detection of some analytes, and, in the future, they will be applied for rapid analysis of different targets.[16,76] In this study, we used fiberglass paper, which has less friction due to a better flow intensity compared to other existing papers such as TLC or filter papers. These patterns designed on paper have microchannels and, due to the capillary flow, the liquid easily passes through it, which helps to identify the analyte easily. To observe the color change, first 10 μL the synthesized NPs were placed in the sensing area, then, the TMB solution and analyte were added, respectively. As shown in the Fig. 7–9, the color change is easily visible and detectable in less than 2 minutes. The images recorded after one hour also have shown the successful construction of hydrophilic channels. According to the UV-vis results, AgNWs had better performance and detection activity in different concentrations of analyte, so they were also selected for further investigation on μPADs. To investigate the effect of acetaldehyde concentration in the real sample, the synthesized AgNWs, first, have dropped on the sensing zone. Then, the different concentration of analyte and

urine was added which the color change was re-detectable. So, this system can be used as a diagnostic kit for clinical studies. Another study performed in this section is related to the capillary power of microchannels. First, 50 μL acetaldehyde was placed in the center of the designed sensor, and the compounds containing AgNWs (probe) and TMB were placed in the sensing area. Over time, discoloration due to the redox reaction can be observed. This color change indicates successful construction of μPADs and paper-based chemo-sensing substrate with excellent pumping ability, low friction, and high flow. In this study, the stability of the prepared microfluidic papers was also tested. According to the results, this system can detect analytes for up to 1 month, which is an excellent and important achievement in the field of paper-based microfluidic biosensors. To this end, the μPADs were functionalized by casting optical detection probe drops for colorimetric analysis of the target ion. After drying at room temperature, the Ag candidate NPs coalesced, and their color turned into green. The drying and combining process take about 10 minutes. Acetaldehyde interactions with the modified μPADs were then assessed for 1 month. After acetaldehyde drop-casting in the sensing zone, it takes about 5 minutes to react with dried nanoparticles to change the color of the nanoparticles to colorless. According to the results, the introduced μPADs were able to detect acetaldehyde within 30 days. This could be the beginning of the development of nanoparticle-modified μPADs for rapid and accurate identification of acetaldehyde. Optical interaction and optical properties between nanoparticles and paper substrates are affected by the aggregation of nanoparticles in cellulose fibers of the paper, the refractive index of paper, and the nanoparticle's spatial location. The penetration and aggregation of nanoparticles in the porous structure of the paper can
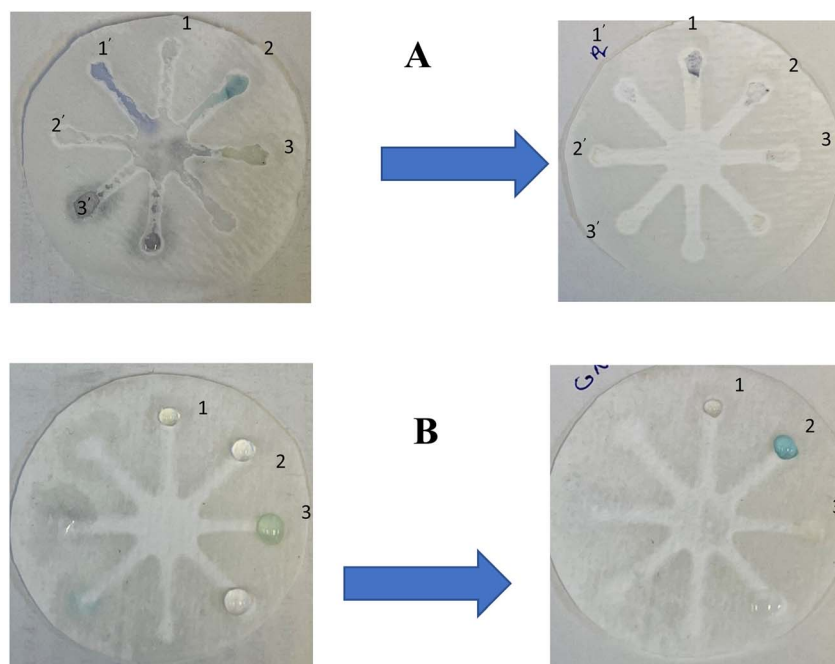

Fig. 7 Photographic images of the microfluidic paper-based calorimetric chemo sensor for reaction systems: (A) AgNWs (zone 1–3), AgNPrs (zone 1′–3′), and (B) AgNPs-Cit (zone 1–3), (1) NPs, (2) NPs + TMB, (3) NPs + TMB + acetaldehyde.
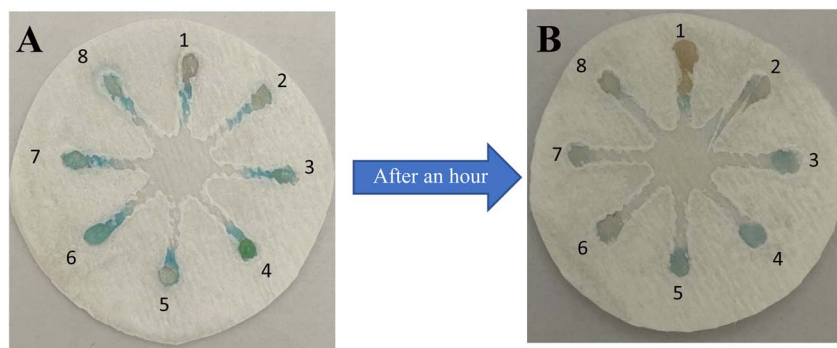
Fig. 8 Photographic images of the (A) different concentration of acetaldehyde and (B) different concentration of acetaldehyde in real sample on the surface of the microfluidic paper-based calorimetric chemo sensor.
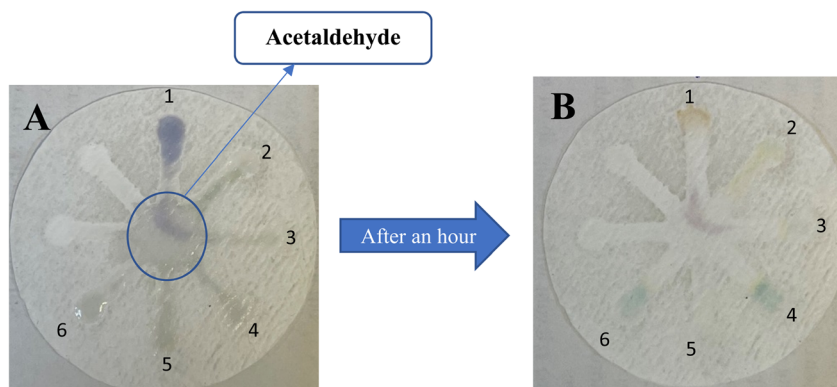

Fig. 9 (A) Photographic images of the microfluidic paper-based calorimetric chemo sensor for evaluation of capillary: AgNPrs and colored TMB solution and AgNPrs (zone 1–2), AgNWs and colored TMB solution and AgNWs (zone 3–4), AgNPs-Cit and colored TMB solution and AgNPs-Cit (zone 5–6). (B) Photographic images of prepared paper after an hour.

cause different light interactions compared to a nonporous flat substrate. Indeed, during drying and aggregation, the global state of the nanoparticles is maintained, which is important for controlling their optical properties. However, the reproducibility of the aggregation and adsorption mode of nanoparticles is limited by the random fibrous structure of the paper substrate.[77] In fact, in this study, acetaldehyde was identified with sufficient accuracy for the first time using μPADs. This technique can be further used to identify other analytes including amino acids. These patterns are designed at a very low price and are simple materials. They are very small in size which helps in easy transportation. Complex laboratory systems are much more expensive, and all tests require skilled operators.

5. Conclusion

In this study, we presented an innovated colorimetric method integrated with UV-vis spectroscopic technique for identifying acetaldehyde in real samples using various types of AgNPs. Also, the paper-based microfluidic device was used in this work, which had excellent stability and reproducibility toward real time colorimetric detection of acetaldehyde in the presence of different interfering agents. In this study, three types of silver

nanoparticles were used. The silver nanowires showed the best colorimetric performance of monitoring of acetaldehyde. This is the first report that shows the specific and sensitive detection of acetaldehyde in real samples using a colorimetric and microfluidic paper-based sensing method. Additionally, due to the outstanding features of this system, it is highly likely that these devices will be commercially available in the near future and will replace complex laboratory methods.

Conflicts of interest

There are no conflicts to declare.

Acknowledgements

References

1 H. Shue, *International affairs*, 1999, vol. 75, pp. 531–545.

2 M. Kumar, H. Chen, S. Sarsaiya, S. Qin, H. Liu, M. K. Awasthi, S. Kumar, L. Singh, Z. Zhang and N. S. Bolan, *J. Hazard. Mater.*, 2021, **409**, 124967.

3 C. S. Lieber, *Biochem. Soc. Trans.*, 1988, **16**, 241–247.

4 C. P. Eriksson, *Alcohol.: Clin. Exp. Res.*, 2001, **25**, 15S–32S.

5 F. Vazart, C. Ceccarelli, N. Balucani, E. Bianchi and D. Skouteris, *Mon. Not. R. Astron. Soc.*, 2020, **499**, 5547–5561.

6 Y. Cao, Z. Teng, J. Zhang, T. Cao, J. Qian, J. Wang, W. Qin and H. Guo, *Sens. Actuators, B*, 2020, **320**, 128354.

7 P. Patil, U. T. Nakate, Y. T. Nakate and R. C. Ambare, *Mater. Sci. Semicond. Process.*, 2019, **101**, 76–81.

8 A. Stornetta, V. Guidolin and S. Balbo, *Cancers*, 2018, **10**, 20.

9 M. Salaspuro, *Visceral medicine*, 2020, vol. 36, pp. 167–174.

10 M. T. Nieminen and M. Salaspuro, *Cancers*, 2018, **10**, 11.

11 M. Hadei, A. Shahsavani, P. K. Hopke, M. Kermani, M. Yarahmadi and B. Mahmoudi, *Environ. Pollut.*, 2019, **254**, 112943.

12 E. Bertheussen, A. Verdaguer-Casadevall, D. Ravasio, J. H. Montoya, D. B. Trimarco, C. Roy, S. Meier, J. Wendland, J. K. Nørskov and I. E. Stephens, *Angew. Chem.*, 2016, **128**, 1472–1476.

13 C. Eriksson, *Mutation Research/Reviews in Genetic Toxicology*, 1987, vol. 186, pp. 235–240.

14 R. Pauliukaite, M. E. Ghica, M. M. Barsan and C. M. Brett, *Anal. Lett.*, 2010, **43**, 1588–1608.

15 H. Aldewachi, T. Chalati, M. Woodroofe, N. Bricklebank, B. Sharrack and P. Gardiner, *Nanoscale*, 2018, **10**, 18–33.

16 P. Abdollahiyan, M. Hasanzadeh, P. Pashazadeh-Panahi and F. Seidi, *J. Mol. Liq.*, 2021, **338**, 117020.

17 P. Abdollahiyan, M. Hasanzadeh, F. Seidi and P. Pashazadeh-Panahi, *J. Environ. Chem. Eng.*, 2021, **9**, 106197.

18 J. Oh, S. Kang, C. G. Lee and M. S. Han, *Analyst*, 2018, **143**, 4592–4599.

19 A. Saadati, S. Hassanpour, M. de la Guardia, J. Mosafer, M. Hashemzaei, A. Mokhtarzadeh and B. Baradaran, *TrAC, Trends Anal. Chem.*, 2019, **114**, 56–68.

20 Q. Zhang, J. Li, Y. Wang, Y. Ma, M. He, D. Zhao, D. Huo, L. Lu and C. Hou, *Anal. Methods*, 2021, **13**, 5478–5486.

21 G. Zilberstein, R. Zilberstein, S. Zilberstein, U. Maor, E. Baskin, S. Zhang and P. G. Righetti, *Electrophoresis*, 2017, **38**, 2168–2174.

22 M. del Mar Darder, M. Bedoya, L. A. Serrano, M. Ángel Alba and G. Orellana, *Sens. Actuators, B*, 2022, **353**, 131099.

23 M. Mahmoudpour, J. E. N. Dolatabadi, M. Torbati and A. Homayouni-Rad, *Biosens. Bioelectron.*, 2019, **127**, 72–84.

24 X. Sun, B. Li, A. Qi, C. Tian, J. Han, Y. Shi, B. Lin and L. Chen, *Talanta*, 2018, **178**, 426–431.

25 C. R. Rao, G. U. Kulkarni, P. J. Thomas and P. P. Edwards, *Chem. Soc. Rev.*, 2000, **29**, 27–35.

26 C. Zhao, M. M. Thuo and X. Liu, *Science and technology of advanced materials*, 2013.

27 E. L. Fava, T. A. Silva, T. M. do Prado, F. C. de Moraes, R. C. Faria and O. Fatibello-Filho, *Talanta*, 2019, **203**, 280–286.

28 D. Lin, B. Li, L. Fu, J. Qi, C. Xia, Y. Zhang, J. Chen, J. Choo and L. Chen, *Microsyst. Nanoeng.*, 2022, **8**, 1–10.

29 J. Qi, B. Li, X. Wang, L. Fu, L. Luo and L. Chen, *Anal. Chem.*, 2018, **90**, 11827–11834.

30 J. Qi, B. Li, X. Wang, Z. Zhang, Z. Wang, J. Han and L. Chen, *Sens. Actuators, B*, 2017, **251**, 224–233.

31 X. Li, C. Zhao and X. Liu, *Microsyst. Nanoeng.*, 2015, **1**, 1–7.

32 F. Liu and C. Zhang, *Sens. Actuators, B*, 2015, **209**, 399–406.

33 F. Farshchi, A. Saadati, M. Hasanzadeh and F. Seidi, *RSC Adv.*, 2021, **11**, 27298–27308.

34 A. Saadati, F. Farshchi, M. Hasanzadeh and F. Seidi, *Anal. Methods*, 2021, **13**, 3909–3921.

35 A. Desireddy, B. E. Conn, J. Guo, B. Yoon, R. N. Barnett, B. M. Monahan, K. Kirschbaum, W. P. Griffith, R. L. Whetten and U. Landman, *Nature*, 2013, **501**, 399–402.

36 C. M. Crisan, T. Mocan, M. Manolea, L. I. Lasca, F.-A. Tăbăran and L. Mocan, *Appl. Sci.*, 2021, **11**, 1120.

37 S. Madersbacher and P. Berger, *J. Immunol. Methods*, 1991, **138**, 121–124.

38 P. D. Josephy, R. P. Mason and T. Eling, *Cancer Res.*, 1982, **42**, 2567–2570.

39 P. Ni, Y. Sun, H. Dai, J. Hu, S. Jiang, Y. Wang and Z. Li, *Biosens. Bioelectron.*, 2015, **63**, 47–52.

40 H.-J. Eom, N. Chatterjee, J. Lee and J. Choi, *Toxicol. Lett.*, 2014, **229**, 311–318.

41 C. V. Restrepo and C. C. Villa, *Environ. Nanotechnol., Monit. Manage.*, 2021, **15**, 100428.

42 F. Farshchi, A. Saadati, N. Fathi, M. Hasanzadeh and M. Samiei, *Anal. Methods*, 2021, **13**, 1286–1294.

43 L. Liu, C. A. Burnyeat, R. S. Lepsenyi, I. O. Nwabuko and T. L. Kelly, *Chem. Mater.*, 2013, **25**, 4206–4214.

44 M. Kudryashov, A. Logunov, D. Gogova, A. Mashin and G. De Filpo, *Opt. Mater.*, 2020, **101**, 109746.

45 J. N. Silva, J. Saade, P. M. Farias and E. H. L. Falcão, *Adv. Nanopart.*, 2013, **2**, 217–222.

46 M. Skiba, A. Pivovarov, A. Makarova and V. Vorobyova, *Chem. J. Mold.*, 2018, **13**, 7–14.

47 Z. Yang, H. Qian, H. Chen and J. N. Anker, *J. Colloid Interface Sci.*, 2010, **352**, 285–291.

48 C. Chen, L. Wang, G. Jiang, J. Zhou, X. Chen, H. Yu and Q. Yang, *Nanotechnology*, 2006, **17**, 3933.

49 N. Korkmaz, K. B. Akar, R. İmamoğlu, D. Kısa and A. Karadağ, *Appl. Organomet. Chem.*, 2021, **35**, e6213.

50 R. Eivazzadeh-Keihan, E. Bahojb Noruzi, K. Khanmohammadi Chenab, A. Jafari, F. Radinekiyan, S. M. Hashemi, F. Ahmadpour, A. Behboudi, J. Mosafer and A. Mokhtarzadeh, *J. Tissue Eng. Regener. Med.*, 2020, **14**, 1687–1714.

51 J. Du, L. Jiang, Q. Shao, X. Liu, R. S. Marks, J. Ma and X. Chen, *Small*, 2013, **9**, 1467–1481.

52 R. Elghanian, J. J. Storhoff, R. C. Mucic, R. L. Letsinger and C. A. Mirkin, *Science*, 1997, **277**, 1078–1081.

53 H. Jiang, Z. Chen, H. Cao and Y. Huang, *Analyst*, 2012, **137**, 5560–5564.

54 A. Ravindran, M. Elavarasi, T. Prathna, A. M. Raichur, N. Chandrasekaran and A. Mukherjee, *Sens. Actuators, B*, 2012, **166**, 365–371.

55 D. Xiong and H. Li, *Nanotechnology*, 2008, **19**, 465502.

56 J. Duan, H. Yin, R. Wei and W. Wang, *Biosens. Bioelectron.*, 2014, **57**, 139–142.

57 V. Brasiliense, A. N. Patel, A. Martinez-Marrades, J. Shi, Y. Chen, C. Combellas, G. Tessier and F. Kanoufi, *J. Am. Chem. Soc.*, 2016, **138**, 3478–3483.

58 S. Smitha, K. Nissamudeen, D. Philip and K. Gopchandran, *Spectrochim. Acta, Part A*, 2008, **71**, 186–190.

59 V. Amendola, O. M. Bakr and F. Stellacci, *Plasmonics*, 2010, **5**, 85–97.

60 L. Mahmudin, E. Suharyadi, A. B. S. Utomo and K. Abraha, *J. Mod. Phys.*, 2015, **6**, 1071.

61 M. Duval Malinsky, K. L. Kelly, G. C. Schatz and R. P. Van Duyne, *J. Phys. Chem. B*, 2001, **105**, 2343–2350.

62 E. Hutter, J. Fendler and D. Roy, *J. Phys. Chem. B*, 2001, **105**, 11159–11168.

63 M. Fan, M. Thompson, M. L. Andrade and A. G. Brolo, *Anal. Chem.*, 2010, **82**, 6350–6352.

64 G. Xu, Y. Chen, M. Tazawa and P. Jin, *J. Phys. Chem. B*, 2006, **110**, 2051–2056.

65 R. Kumar, K. Prakash, P. Cheang and K. Khor, *Langmuir*, 2004, **20**, 5196–5200.

66 Z. Qu, P. Duan, J. Zhou, Y. Wang and M. Liu, *Nanoscale*, 2018, **10**, 985–991.

67 C. Liu, Q. Pang, T. Wu, W. Qi, W. Fu and Y. Wang, *J. Anal. Test.*, 2021, **5**, 210–216.

68 C. Liu, Q. Li, C. Niu, F. Zheng and Y. Zhao, *J. Sci. Food Agric.*, 2018, **98**, 4733–4741.

69 B. Liang, Y. Liu, Y. Zhao, T. Xia, R. Chen and J. Yang, *Biosens. Bioelectron.*, 2021, **193**, 113566.

70 L. Zhang, M. Zhou and S. Dong, *Anal. Chem.*, 2012, **84**, 10345–10349.

71 A. Chaubey, M. Gerard, R. Singhal, V. Singh and B. Malhotra, *Electrochim. Acta*, 2001, **46**, 723–729.

72 A. Avramescu, T. Noguer, M. Avramescu and J.-L. Marty, *Anal. Chim. Acta*, 2002, **458**, 203–213.

73 A. Avramescu, S. Andreescu, T. Noguer, C. Bala, D. Andreescu and J.-L. Marty, *Anal. Bioanal. Chem.*, 2002, **374**, 25–32.

74 Y.-Q. Liu, B. Ji, X.-H. Yan, S. Lv, F. Fang, X.-L. Guo and Z.-Y. Wu, *Microchem. J.*, 2022, **174**, 107041.

75 L. Wang, B. Li, J. Wang, J. Qi, J. Li, J. Ma and L. Chen, *J. Hazard. Mater.*, 2022, **428**, 128165.

76 S. Hassanpour, M. Hasanzadeh, A. Saadati, N. Shadjou, J. Soleymani and A. Jouyban, *Microchem. J.*, 2019, **146**, 345–358.

77 Y. H. Ngo, D. Li, G. P. Simon and G. Garnier, *Adv. Colloid Interface Sci.*, 2011, **163**, 23–38.